第 43 卷 第 22 期/2023 年 11 月/光学学报 研究论文

光学学报

基于光纤随机激光的1.7 μm波段高功率涡旋光束产生

于观玉[1]，张春香[2]，黄政[3]，刘锐[3]，马瑞[1]，白志勇[3]，范滇元[1]，刘军[1*]

[1]深圳大学微纳光电子学研究院二维材料光电科技国际合作联合实验室，广东 深圳 518060；

[2]深圳技术大学工程物理学院，广东 深圳 518118；

[3]深圳大学物理与光电工程学院光纤传感技术粤港联合研究中心，广东 深圳 518060

摘要 1.7 μm激光处于眼安全波段并位于许多重要气体分子的指纹吸收峰，在生物医疗、气体传感等领域具有重要应用价值。而涡旋光束作为一种新兴的结构光场，其具有环形光强分布和螺旋相位波前，并携带轨道角动量，在光通信、微粒操控等领域应用广泛。因此发展1.7 μm高能涡旋激光器具有重要的研究价值和应用前景。但传统稀土离子掺杂光纤或晶体的发射谱，或难以覆盖该波段，或在该波段激光增益较小，且涡旋光产生主要基于空间光结构，导致1.7 μm波段涡旋光激光系统复杂、集成度低，难以实现高功率输出。本文利用螺旋长周期光纤光栅作为涡旋模式转换器，在基于受激拉曼散射效应的1.7 μm波段光纤随机激光半开放腔中实现了全光纤结构的高功率涡旋激光输出，最大输出功率为2.09 W，中心波长为1690 nm。得益于涡旋光纤随机激光器的全光纤结构，该装置具有良好的时域稳定性，短时时域波动低至2.8%。该研究结果不仅为实现兼具高功率输出和良好时域稳定性的紧凑型1.7 μm波段涡旋激光器提供有效方案，还能进一步拓展其在激光医疗、气体检测、光镊和生物成像等领域的应用。

关键词 1.7 μm波段；涡旋光束；光纤随机激光器；螺旋长周期光纤光栅；涡旋光纤随机激光器

中图分类号 TN248 **文献标志码** A **DOI**：10.3788/AOS231203

1 引 言

1.7 μm激光处于眼安全波段，对水分子吸收较不敏感但却位于脂肪、胶原蛋白等大分子的主要吸收峰，同时也覆盖了多种气体、有机物的吸收线。因此，该波段激光在生物医疗、气体传感、光学成像等领域具有重要应用前景[1-2]。另一方面，涡旋光束是一种具有螺旋相位波前和携带轨道角动量的特殊结构光场[3-4]，它的独特性质使其在自由空间光通信、微粒操控、光学成像等领域具有广阔的发展前景[5-7]。因此，开展1.7 μm波段涡旋激光的高效产生机理及其特性调控技术研究能进一步拓宽1.7 μm激光和涡旋光束的应用领域和范围，具有重要的科学意义和应用价值。

涡旋光束的产生方案主要分为两类：1)在自由空间中利用螺旋相位板、空间光调制器、q波片、超表面等相位型器件来产生[8-10]；2)在光纤等波导结构中利用少模布拉格光纤光栅、长周期光纤光栅和模式选择耦合器等模式选择器件来激发涡旋光束[11-13]。关于涡旋激光器的研究有很多，但是目前报道的工作波段主要集中在可见光及1 μm、1.5 μm近红外波段[14-16]，1.7 μm波段高功率涡旋激光器还很少涉及，原因主要在于缺乏实现1.7 μm波段激光高效输出的稀土离子掺杂有源增益光纤和增益晶体。此外，掺铋光纤、铥铋共掺光纤等特种光纤制作工艺不成熟、成本较为高昂，且输出功率较低[17-19]。而光纤随机激光器(RFL)作为一种特殊的无谐振激光器[20-21]，具有结构简单、成本低廉[22]、易于实现高功率高效率输出[23]、良好的时域稳定性[24]、低相干性[25]等优点，是实现1.7 μm波段高性能激光的优良技术途径。

特别是，基于光纤随机激光的柱矢量光束和涡旋光束的产生方案也越来越受到众多研究人员的关注，目前相关研究工作已有许多报道。Wang等[26]报道了利用模式选择耦合器在光纤随机激光器中实现了1030 nm柱矢量光束。Lv等[27]基于模式注入锁定技术实现了空间振荡模式可切换的1056 nm光纤随机激光输出。Ma等[28]报道了一种基于空间光调制器的轨道

收稿日期：2023-06-30；**修回日期**：2023-08-05；**录用日期**：2023-09-04；**网络首发日期**：2023-09-14

基金项目：广东省基础与应用基础研究基金(2022A1515010326，2021A1515011532，2020A1515110471，2020A1515111143)、深圳市科创委优青项目(RCYX20210609103157071)、深圳市科创委重点项目(JCYJ20220818100019040)、深圳技术大学新引进高端人才财政补助科研启动项(GDRC202138)

通信作者：*liu-jun-1987@live.cn

角动量模式可控的1092 nm涡旋光纤随机激光器。Lei等[29]研究了基于空间光调制器的1583 nm涡旋光纤随机激光器的相干特性。然而，基于光纤随机激光实现1.7 μm波段高功率涡旋光束输出的研究还鲜有涉及，一方面由于基于自由空间的涡旋激光器结构较为复杂、系统集成度低且光学损耗较大，难以获得高功率涡旋光输出，另一方面是所采用的模式转换器件存在固有缺陷，如插入损耗高、模式转换效率低、损伤阈值低等。相比于模式选择耦合器，螺旋长周期光纤光栅具有更低的插入损耗、更高的模式转换效率；相比于空间光调制器，它具有较高的损伤阈值，且有利于实现全光纤结构、提高系统集成度[30]。因此，本文选择螺旋长周期光纤光栅作为光纤随机激光的模式转换器来实现1.7 μm波段高功率涡旋激光输出。

本文提出一种基于光纤随机激光及螺旋长周期光纤光栅的全光纤结构涡旋激光产生方案，实验实现了1.7 μm波段高功率涡旋激光输出，最大输出功率为2.09 W，中心波长为1690 nm。此外，获得的1.7 μm波段涡旋随机激光展现出良好的时域稳定性，短时时域波动低至2.8%。该研究工作可为实现兼具高功率输出和良好时域稳定性的1.7 μm波段涡旋激光器提供可行的技术路线，进一步拓展其在激光医疗、气体检测、光镊和生物成像等领域的应用。

2 实验结构

1.7 μm波段高功率涡旋光纤随机激光器的实验装置图如图1所示。实验装置包含1566 nm光纤随机激光器泵浦源、1.7 μm波段光纤随机激光器、涡旋光束产生和检测装置三个部分。第一，1566 nm光纤随机激光器泵浦源为主振荡功率放大器(MOPA)结构，包含1566 nm光纤随机激光种子光和功率放大器两部分。光纤随机激光种子光采用后向泵浦的半开放腔结构，考虑到光纤随机激光种子光源的输出时域稳定性，其输出功率被设置为1.5 W，并将其输出末端直接与功率放大器级连接。在功率放大器级，976 nm激光二极管通过(2+1)×1的信号/泵浦合束器(Combiner，最大承受功率为50 W)泵浦长度为4 m的多模铒镱共掺光纤(MM-EYDF-12/130-HE，Nufern，美国)；包含包层功率剥除器(CPS)和模场适配器(MFA)的集成光纤器件熔接在多模铒镱共掺光纤尾端，用来剥离未吸收的泵浦光和降低不同尺寸光纤熔接时引入的插入损耗；高功率光学隔离器(最大承受功率为20 W)熔接在集成光纤器件末端，以防止激光回返损坏腔内器件。第二，1.7 μm波段光纤随机激光器采用前向泵浦的半开放腔结构，激光泵浦由建立的1566 nm光纤随机激光器泵浦源提供，其输出末端直接熔接1690 nm高反光纤布拉格光栅(HR-FBG，反射率为99%，3 dB带宽为0.2 nm)。激光增益由熔接在1690 nm高反光纤布拉格光栅后面的4 km标准单模光纤(SMF，G. 652D)提供；激光反馈由4 km单模光纤中随机分布的瑞利散射和1690 nm高反光纤布拉格光栅的点式反射提供；为消除光纤端面菲涅耳反射影响，所有输出端口的尾部均做斜角切割处理。第三，在涡旋光束产生和检测装置部分，50∶50的耦合器将1.7 μm波段光纤随机激光器输出光分成两束，一束被自制的1.7 μm螺旋长周期光纤光栅直接转换成涡旋光，另一束作为参考高斯光束。涡旋光束和参考高斯光束在分光镜上重合并发生干涉，从而解调所获得的1.7 μm涡旋随机激光的螺旋相位。实验中采用功率计(919P-250-35，Newport，美国)、光谱分析仪(AQ6375B，Yokogawa，日本)、射频频谱分析仪(N9322C，Keysight，美国)、示波器(MDO3054，Tektronix，美国)、光电探测器(DET10D2，Thorlab，美国，带宽为14 MHz)和电荷耦合器件(CCD，bGS-USB-SP928-OSI，Spiricon，美国)来测量输出1.7 μm波段涡旋随机激光器的输出特性。所有激光器件置于温度设定为20 ℃的水冷板上来避免产生的热负荷对激光器件的损伤和提升系统稳定性。

3 实验结果与讨论

实验首先测量了建立的1.7 μm波段光纤随机激光器输出特性。图2(a)给出了其1.7 μm光纤随机激光输出功率同1566 nm泵浦功率及剩余泵浦功率的变化关系。当泵浦功率低于激光泵浦阈值3.01 W时，未有1.7 μm波段随机激光激射，剩余泵浦功率线性增加；当泵浦功率大于3.01 W激光阈值时，1.7 μm波段光纤随机激光开始产生，随着泵浦功率进一步增加，剩余泵浦功率不断下降，1566 nm泵浦光逐渐转换为1.7 μm波段随机激光；当最大泵浦功率为11.96 W时，1.7 μm波段光纤随机激光器的最大输出功率为7.98 W。在整个泵浦功率范围未出现明显激光饱和，可通过简单地增加泵浦功率进一步提升1.7 μm波段光纤随机激光输出功率。1.7 μm波段光纤随机激光的功率占比(1.7 μm波段激光功率与激光器输出总功率的比值)及光光转换效率与泵浦功率的关系如图2(b)所示。当泵浦功率低于激光泵浦阈值3.01 W时，1.7 μm波段光纤随机激光器的功率占比和光光转换效率几乎为0；当泵浦功率超过激光阈值后，随着泵浦功率的提升1.7 μm波段激光功率占比和光光转换效率线性增加；当泵浦功率超过6.03 W后，其功率占比和光光转换效率增速逐渐趋于饱和，在最大泵浦功率为11.96 W时，1.7 μm波段激光功率占比大于99%，光光转换效率为67%。不同输出功率下的1.7 μm波段光纤随机激光输出光谱演变如图2(c)所示。1.7 μm波段光纤随机激光器输出光谱中心波长主要由高反光纤布拉格光栅的中心波长决定，为1690 nm。当1.7 μm波段光纤随机激光未产生时，输出光谱仅有1566 nm泵浦光；随着输出功率增加，1566 nm泵浦光

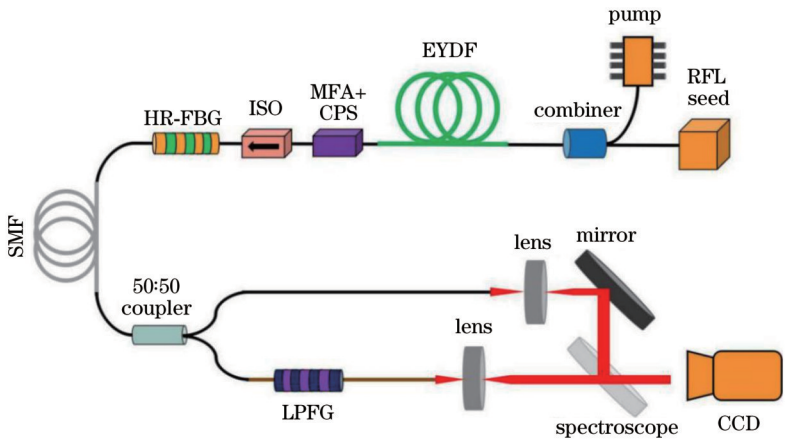

RFL seed: 1566 nm fiber random laser seed light; pump: 976 nm laser diode pump source; combiner: beam combiner; EYDF: erbium ytterbium co doped fiber; MFA: mode field adapter; CPS: cladding pump stripper; ISO: optical isolator; HR-FBG: 1690 nm high reflectivity fiber Bragg grating; SMF: standard single mode fiber; coupler: coupler; LPFG: long period fiber grating; lens: lens; mirror: mirror; spectroscope: spectroscope; CCD: charge coupled device

图 1　1.7 μm 波段高功率涡旋光纤随机激光器实验装置图

Fig. 1　Experimental setup of the 1.7 μm high-power vortex RFL

开始向 1690 nm 随机激光转化，对应泵浦光谱尖峰强度变低 1690 nm 输出光谱强度逐渐增加。

为实现高性能涡旋随机激光输出，实验中采用螺旋长周期光纤光栅作为光纤模式选择和转换器件，将产生的随机激光直接转换成对应参数的涡旋光输出。螺旋长周期光纤光栅由二氧化碳激光器在传统单模光纤上刻写，耦合产生的对应轨道角动量模式即为涡旋光，但其属于光纤包层模，难以实现长距离传输[31-32]。因此需在螺旋长周期光纤光栅输出尾端熔接一段少模环芯光纤来实现涡旋光束的长距离传输。图 3(a)给出了 1.7 μm 波段螺旋长周期光纤光栅的透射光谱。当中心波长为 1690 nm 时，螺旋长周期光纤光栅从高

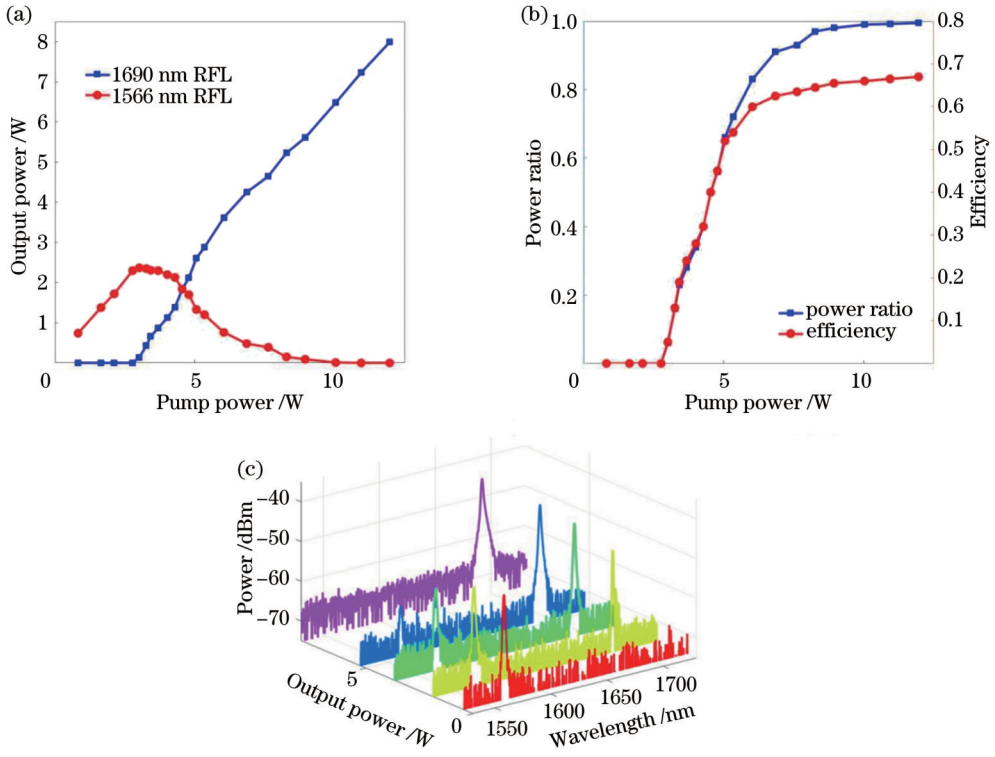

图 2　1.7 μm 波段光纤随机激光器输出特性实验结果。(a)输出功率和残余泵浦功率与泵浦功率关系图；(b)功率占比和光光转换效率与泵浦功率关系图；(c)不同输出功率下的光谱演变图

Fig. 2　Experimental results of output characteristics of the 1.7 μm band fiber random laser. (a) Relationship between output power and residual pump power and the pump power; (b) relationship between power ratio and optical to optical conversion efficiency and the pump power; (c) evolution of output spectrum with different output powers

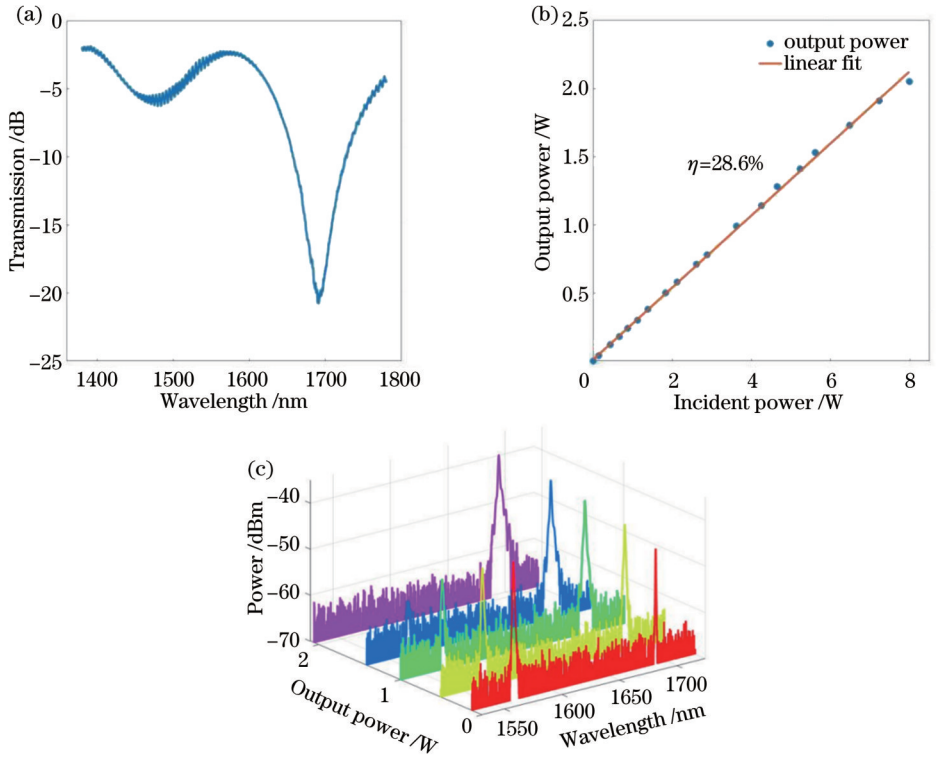

图 3　1.7 μm 波段涡旋光纤随机激光器输出特性实验结果。(a)螺旋长周期光纤光栅透射光谱图;(b)输出功率和斜效率与入射光功率关系图;(c)不同输出功率下的光谱演变图

Fig. 3　Experimental results of output characteristics of the 1.7 μm band vortex RFL. (a) Transmission spectrum of the spiral LPFG; (b) relationship between output power and slope efficiency and incident power; (c) evolution of the output spectrum with different output powers

斯基模转换到一阶涡旋光束的模式转换效率约为 97%(对应于 16 dB 模式转换效率)。将 1.7 μm 波段光纤随机激光器输出端与螺旋长周期光纤光栅熔接从而实现全光纤结构的 1.7 μm 波段涡旋光纤随机激光输出。首先,涡旋光纤随机激光器的输出功率和斜效率与入射光功率的关系如图 3(b)所示。随着入射光功率的增加,涡旋光纤随机激光输出功率也同步线性增加。当入射光功率达到最高功率 7.96 W 时,涡旋光纤随机激光器的最大输出功率为 2.09 W,对应斜效率为 28.6%。1.7 μm 波段光纤随机激光未能彻底转化为涡旋光,其主要原因在于:1)螺旋长周期光纤光栅缺乏有效的热管理;2)刻写螺旋长周期光纤光栅的单模光纤与少模环芯光纤的熔接损耗;3)在螺旋长周期光纤光栅中通过涡旋模式耦合所获得的耦合轨道角动量模式属于单模光纤的包层模,难以支持涡旋光束的长距离传输,在传输过程中会受到较大损耗。1.7 μm 波段涡旋光纤随机激光器的输出功率的进一步提升有望通过增加入射光功率和替换性能更好的螺旋长周期光纤光栅来实现。1.7 μm 波段涡旋光纤随机激光器在不同输出功率下的光谱演化图(分辨率为 0.5 nm)如图 3(c)所示。结果表明,涡旋光纤随机激光器的输出光谱中心波长仍为 1690 nm,其在不同输出功率下的光谱演化图与 1690 nm 光纤随机激光器输出光谱基本一致。

输出 1.7 μm 波段涡旋光纤随机激光的拓扑荷检测实验装置如图 1 中下半部分所示,为典型的马赫-曾德尔干涉仪,输出的 1690 nm 光纤随机激光被一个 3 dB 耦合器分成两路,上面一路作为参考高斯光束,下面一路由一个 1.7 μm 波段螺旋长周期光纤光栅直接转换成涡旋光束。图 4(d)为参考高斯光束的模场图,其强度分布表现为典型的高斯光束分布。与此同时,图 4(e)为待检测的信号光束,其强度分布呈现典型的涡旋光束分布,光场强度呈现甜甜圈状分布。然后,参考高斯光束与涡旋光束这两束光在分光镜上相互叠加并发生干涉,得到的干涉图可以解调输出的涡旋光束的相位。涡旋光纤随机激光器的干涉图样如图 4(f)所示,其干涉图样呈一个螺旋分布,说明涡旋光纤随机激光器输出的涡旋光束拓扑荷为一阶。参考高斯光束、待检测涡旋光束、涡旋光束干涉图样的理论仿真光场强度分布图如图 4(a)~(c)所示,实验所测得的参考高斯光束、待检测涡旋光束、涡旋光束干涉图样的光场强度分布图与理论仿真结果实现较好的符合。

最后,实验测量了 1.7 μm 波段涡旋光纤随机激光器在最大输出功率 2.09 W 时的输出特性。图 5(a)为涡旋光纤随机激光器的短时时域波动情况,可以看出,其短时时域波动较小(输出强度波动 std/mean 值为 2.8%),表明 1.7 μm 波段全光纤结构涡旋光纤随机激

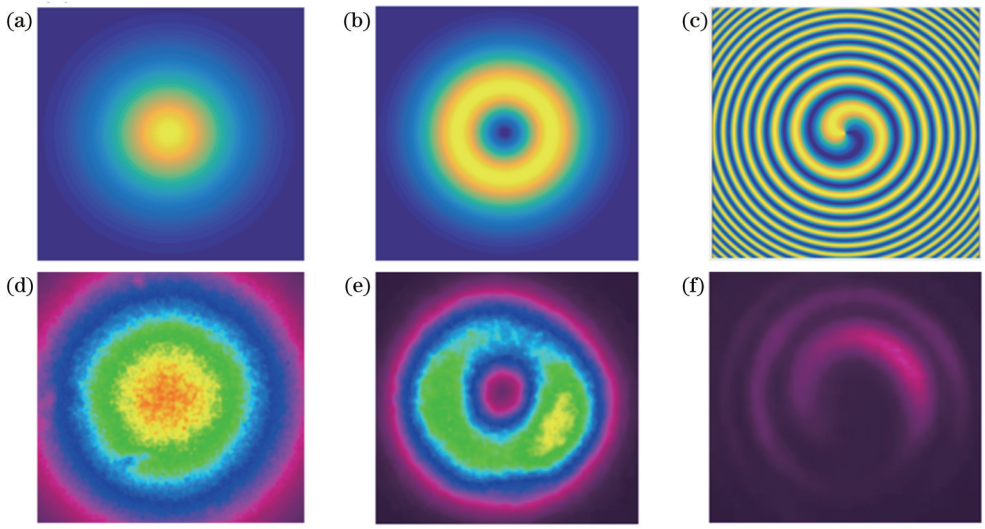

图 4 参考高斯光束、一阶涡旋光束、一阶涡旋光束和参考高斯球面波的干涉模式的光场强度分布图的理论仿真结果和实验测量结果。(a)~(c)理论仿真结果;(d)~(f)实验测量结果

Fig. 4 Theoretical simulation results and experimental measurement results of the intensity profiles of reference Gaussian beam, first order vortex beam, interference pattern between first order vortex beam, and reference Gaussian spherical wave. (a)-(c) Theoretical simulation results; (d)-(f) experimental measurement results

光器具有良好的时域稳定性。此外,涡旋光纤随机激光器的射频频谱如图 5(b)所示,与光电探测器固有的信号噪声响应相比较可以看出,在整个频率范围内只有少量的低频分量,没有明显的纵模频率分量,无谐振频率的射频频谱是光纤随机激光器的固有特征,表明建立的 1.7 μm 波段涡旋光纤随机激光器能很好地保持光纤随机激光器的特性[24,33],包括良好的时域稳定性和无谐振模式输出。

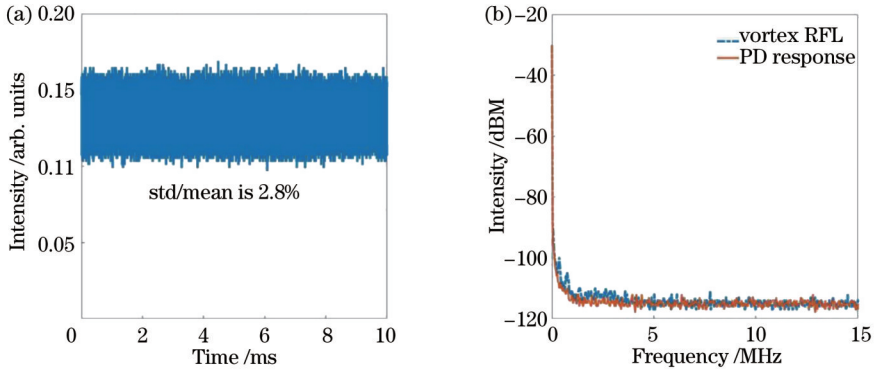

图 5 涡旋光纤随机激光器。(a)短时时域图;(b)射频频谱图

Fig. 5 Vortex RFL. (a) Short time temporal trace; (b) radio frequency spectrum

4 结 论

本文提出一种全光纤结构的 1.7 μm 波段高功率涡旋光纤随机激光器。基于光纤随机激光的半开放腔和螺旋长周期光纤光栅实现了 1.7 μm 波段全光纤结构的高功率涡旋随机激光输出,最大输出功率为 2.09 W,中心波长为 1690 nm。获得的涡旋光纤随机激光具有良好的时域稳定性、较低的相对强度扰动以及无模式振荡输出,短时时域波动低至 2.8%。通过增加 1.7 μm 波段光纤随机激光注入功率和替换性能更好的螺旋长周期光纤光栅有望进一步提升涡旋光纤随机激光器的输出功率。更高阶拓扑荷输出的涡旋光纤随机激光器可通过简单替换对应阶数的螺旋长周期光纤光栅来实现。该研究工作为实现高性能 1.7 μm 波段涡旋激光器提供了有效的方案,有望应用于激光医疗、气体检测、光镊和生物成像等领域。

参 考 文 献

[1] Zhang L, Zhang J X, Sheng Q, et al. Intracavity tandemly-pumped and gain-switched Tm-doped fiber laser at 1.7 μm[J]. Journal of Lightwave Technology, 2022, 40(13): 4373-4378.

[2] Ma R, Quan X, Zhao T, et al. Robust 1.69 μm random fiber laser with high spectral purity based on ordinary fibers[J]. Journal of Lightwave Technology, 2022, 40(12): 3942-3946.

[3] Dennis M R, O'Holleran K, Padgett M J. Singular optics: optical vortices and polarization singularities[M]//Progress in

optics. Amsterdam: Elsevier, 2009: 293-363.
[4] Allen L, Beijersbergen M W, Spreeuw R J, et al. Orbital angular momentum of light and the transformation of Laguerre-Gaussian laser modes[J]. Physical Review A, 1992, 45(11): 8185-8189.
[5] Milione G, Lavery M P J, Huang H, et al. 4 × 20 Gbit/s mode division multiplexing over free space using vector modes and a q-plate mode (de)multiplexer[J]. Optics Letters, 2015, 40(9): 1980-1983.
[6] Shen Y J, Wang X J, Xie Z W, et al. Optical vortices 30 years on: OAM manipulation from topological charge to multiple singularities[J]. Light: Science & Applications, 2019, 8: 90.
[7] Ren H R, Briere G, Fang X Y, et al. Metasurface orbital angular momentum holography[J]. Nature Communications, 2019, 10: 2986.
[8] Schemmel P, Pisano G, Maffei B. A modular spiral phase plate design for orbital angular momentum generation at millimetre wavelengths[J]. Optics Express, 2014, 22(12): 14712-14726.
[9] Huang T D, Lu T H. Controlling an optical vortex array from a vortex phase plate, mode converter, and spatial light modulator [J]. Optics Letters, 2019, 44(16): 3917-3920.
[10] Gregg P, Mirhosseini M, Rubano A, et al. Q-plates as higher order polarization controllers for orbital angular momentum modes of fiber[J]. Optics Letters, 2015, 40(8): 1729-1732.
[11] Du X Y, Zhang H W, Ma P F, et al. Spatial mode switchable fiber laser based on FM-FBG and random distributed feedback [J]. Laser Physics, 2015, 25(9): 095102.
[12] Huang Y P, Shi F, Wang T, et al. High-order mode Yb-doped fiber lasers based on mode-selective couplers[J]. Optics Express, 2018, 26(15): 19171-19181.
[13] Zhao Y H, Wang T X, Mou C B, et al. All-fiber vortex laser generated with few-mode long-period gratings[J]. IEEE Photonics Technology Letters, 2018, 30(8): 752-755.
[14] 刘俊, 王健. 涡旋光激光器研究进展[J]. 中国激光, 2022, 49(12): 1201001.
Liu J, Wang J. Research progress of vortex laser[J]. Chinese Journal of Lasers, 2022, 49(12): 1201001.
[15] Zhang Z C, Hai L, Fu S Y, et al. Advances on solid-state vortex laser[J]. Photonics, 2022, 9(4): 215.
[16] 连天虹, 杨磊, 朱家华, 等. 微片 Nd∶YAG 涡旋光激光器研究[J]. 光学学报, 2022, 42(21): 2114002.
Lian T H, Yang L, Zhu J H, et al. Study on microchip Nd∶YAG vortex laser[J]. Acta Optica Sinica, 2022, 42(21): 2114002.
[17] Huang M L, Wu J D, Hong J H, et al. High energy switchable pulsed High-order Mode beams in a mode-locking Raman all-fiber laser with high efficiency[J]. Optics Express, 2021, 29(24): 40538-40546.
[18] Xia F, Zhao Y, Hu H F, et al. Broadband generation of the first-order OAM modes in two-mode fiber by offset splicing and fiber rotating technology[J]. Optics & Laser Technology, 2019, 112: 436-441.
[19] Guo L J, Feng Z Q, Fu Y T, et al. Generation of vector beams array with a single spatial light modulator[J]. Optics Communications, 2021, 490: 126915.
[20] Turitsyn S K, Babin S A, Churkin D V, et al. Random distributed feedback fibre lasers[J]. Physics Reports, 2014, 542 (2): 133-193.
[21] 杨茜, 周泽中, 刘恺, 等. 频率间隔可切换多波长布里渊随机光纤激光器[J]. 中国激光, 2022, 49(11): 1101003.
Yang Q, Zhou Z Z, Liu K, et al. Frequency interval switchable multi-wavelength Brillouin random fiber laser[J]. Chinese Journal of Lasers, 2022, 49(11): 1101003.
[22] Wang Z N, Wu H, Fan M Q, et al. High power random fiber laser with short cavity length: theoretical and experimental investigations[J]. IEEE Journal of Selected Topics in Quantum Electronics, 2015, 21(1): 0900506.
[23] Zhang H W, Huang L, Song J X, et al. Quasi-kilowatt random fiber laser[J]. Optics Letters, 2019, 44(11): 2613-2616.
[24] Han B, Rao Y J, Wu H, et al. Low-noise high-order Raman fiber laser pumped by random lasing[J]. Optics Letters, 2020, 45 (20): 5804-5807.
[25] Ma R, Rao Y J, Zhang W L, et al. Multimode random fiber laser for speckle-free imaging[J]. IEEE Journal of Selected Topics in Quantum Electronics, 2019, 25(1): 0900106.
[26] Wang J H, Chen R S, Yao J N, et al. Random distributed feedback fiber laser generating cylindrical vector beams[J]. Physical Review Applied, 2019, 11(4): 044051.
[27] Lv J L, Li H X, Zhang Y M, et al. Few-mode random fiber laser with a switchable oscillating spatial mode[J]. Optics Express, 2020, 28(26): 38973-38982.
[28] Ma X Y, Ye J, Zhang Y, et al. Vortex random fiber laser with controllable orbital angular momentum mode[J]. Photonics Research, 2021, 9(2): 266-271.
[29] Lei H L, Wu J D, Huang M L, et al. Low-spatial coherence vortex beam generation by random distributed feedback fibre laser[J]. Optik, 2022, 268: 169779.
[30] Han Y, Liu Y G, Wang Z, et al. Controllable all-fiber generation/conversion of circularly polarized orbital angular momentum beams using long period fiber gratings[J]. Nanophotonics, 2018, 7(1): 287-293.
[31] Chen J Y, Bai Z Y, Zhu G X, et al. Femtosecond laser inscribed helical long period fiber grating for exciting orbital angular momentum[J]. Optics Express, 2022, 30(3): 4402-4411.
[32] Bai Z Y, Wang Y P, Zhang Y, et al. Helical long-period fiber gratings as wavelength-tunable orbital angular momentum mode generators[J]. IEEE Photonics Technology Letters, 2020, 32 (7): 418-421.
[33] Ma R, Liu J, Fang Z Q, et al. Mid-infrared random fiber laser assisted by the passive feedback[J]. Journal of Lightwave Technology, 2021, 39(15): 5089-5095.

1.7 μm High-Power Vortex Beam Generation Based on Random Fiber Lasers

Yu Guanyu[1], Zhang Chunxiang[2], Huang Zheng[3], Liu Rui[3], Ma Rui[1], Bai Zhiyong[3], Fan Dianyuan[1], Liu Jun[1*]

[1]*International Collaborative Laboratory of 2D Materials for Optoelectronics Science and Technology of Ministry of Education, Shenzhen University Institute of Microscale Optoelectronics, Shenzhen* 518060, *Guangdong, China*;
[2]*College of Engineering Physics, Shenzhen Technology University, Shenzhen* 518118, *Guangdong, China*;
[3]*Guangdong and Hong Kong Joint Research Centre for Optical Fibre Sensors, College of Physics and Optoelectronic Engineering, Shenzhen University, Shenzhen* 518060, *Guangdong, China*

Abstract

Objective Since 1.7 μm lasers are located in the eye-safe wavelength band and also within the fingerprint absorption peaks of many important gas molecules, they have potentially important applications in biomedical, gas sensing, and other fields. Meanwhile, as a novel structured light field, vortex beams can have unique features like annular light intensity distribution, helical phase wavefront, and orbital angular momentum. Therefore, developing high-performance 1.7 μm vortex lasers and investigating involved technologies can further expand the application fields of the lasers, providing scientific significance and application prospects. It is generally difficult for traditional rare-earth-ion doped fibers and crystals to cover the 1.7 μm emission band, or they can only have very weak laser gain in this wavelength band. Additionally, the vortex beam generation usually relies on a free-space lasing structure. These factors ultimately result in a complex vortex lasing configuration operating in the 1.7 μm band with extremely poor integration and low output power. Thus, we employ a helical long-period fiber grating as a vortex mode converter, and propose a high-power all-fiber vortex laser based on a 1.7 μm random fiber laser (RFL) with half-opened cavity, producing a maximum output power of 2.09 W at 1690 nm. Benefiting from the all-fiber structure of the vortex RFL, the laser output shows excellent temporal stability with a short-term temporal fluctuation as low as 2.8%. The results can not only provide a feasible approach to achieve a compact 1.7 μm high-power vortex laser with excellent temporal stability, but also further expand its applications in laser medicine, gas detection, optical tweezers, biological imaging, and other fields.

Methods First, a 1.7 μm high-power RFL is constructed based on the stimulated Raman scattering effect. Then, a helical long-period fiber grating is adopted as a vortex mode converter with the vortex mode conversion efficiency of about 97% corresponding to 16 dB, which can convert the 1.7 μm random lasing into a first-order vortex beam. In this sense, a 1.7 μm high-power vortex RFL with an all-fiber structure is achieved, with the maximum output power of 2.09 W and central wavelength of 1690 nm. Benefiting from the all-fiber structure of the vortex RFL, the whole lasing system has a compact configuration with sound integration and simple thermal management and thus can achieve high-power vortex beam output. Additionally, the vortex RFL shows excellent temporal stability (short-time temporal fluctuation as low as 2.8%), modeless resonant output, and low relative fluctuations. It is expected that the output power of the vortex RFL can be further enhanced by increasing the incident power of the 1.7 μm RFL and optimizing the performance of the helical long-period fiber grating.

Results and Discussions The 1.7 μm high-power vortex random lasing is realized based on a 1.7 μm RFL and a helical long-period fiber grating. The maximum output power is 2.09 W and the central wavelength is 1690 nm (Fig. 3). Furthermore, Fig. 3(b) shows the relationship between the output power and the slope efficiency of the 1.7 μm vortex RFL and the incident power. The output power of the vortex RFL increases almost linearly without obvious saturation signs for the whole power scaling range. By increasing the injection power of the 1.7 μm RFL and replacing the helical long-period fiber grating with better performance, the output power of vortex RFL can be further enhanced. Meanwhile, the topological charge of the vortex RFL is characterized based on a homemade Mach-Zender interferometer, where the vortex laser output is interfered with a reference beam (or the spherical wave). The topological charge is measured to be one, which means the first-order vortex beam (Fig. 4). Finally, the short-time lasing characteristics and the radio frequency (RF) spectrum of the 1.7 μm vortex RFL at the highest output power of 2.09 W are measured. Thanks to the inherent excellent temporal stability and modeless resonant output characteristics of random fiber lasing, the 1.7 μm vortex lasing output inherits the intrinsic advantages of RFL, exhibiting very low short-time temporal fluctuations of 2.8% without resonant cavity frequencies in the RF spectrum (Fig. 5).

Conclusions We propose a 1.7 μm high-power vortex RFL with an all-fiber structure. The 1.7 μm high-power vortex

RFL is realized based on a RFL with a half-open cavity and the helical long-period fiber grating. The maximum output power is 2.09 W and the central wavelength is 1690 nm. The vortex RFL shows excellent temporal stability, low relative intensity fluctuation, and modeless oscillation output. The short-time temporal fluctuations are as low as 2.8%. By increasing the injection power of the 1.7 μm RFL and replacing the helical long-period fiber grating with better performance, the output power of the vortex RFL can be further increased. The vortex RFL with higher topological charges can be realized by simply replacing the corresponding helical long-period fiber grating. This work provide a feasible scheme for the realization of high-performance 1.7 μm vortex lasers, which is expected to be applied to laser medicine, gas detection, optical tweezers, and bio-imaging fields.

Key words 1.7 μm band; vortex beam; random fiber laser; helical long-period fiber grating; vortex random fiber laser